Agronomy Research **12**(2), 341–350, 2014

Influence of the drop size of bioethanol fuel in air-fuel mixture on combustion process of spark ignition engine

R. Ilves*, A. Küüt, T. Kikas and J. Olt

Institute of Technology, Estonian University of Life Sciences, Kreutzwaldi 56, EE51014 Tartu, Estonia; *Correspondence: risto.ilves@emu.ee

Abstract: Bioethanol is widely used as a fuel in spark ignition engines. Brazil and USA are among the largest producers of bioethanol in the world. In order to widen the use of bioethanol as a fuel in spark ignition engines, the combustion process has to be improved. This can be accomplished by dosing bioethanol air-fuel mixture into the engine. Thus, the smaller drop size of the fuel can be achieved than in the air-fuel mixtures formed in regular fuel supply systems. Decreasing the size of the fuel drops decreases evaporation time of the air-fuel mixture and therefore, increases the combustion velocity of the air-fuel mixture. This article gives an overview of using 96.4% bioethanol as a fuel in spark ignition engines when the fuel drop size in the air-fuel mixture directed to cylinder is smaller than in the air-fuel mixture formed in regular fuel supply systems. Results indicate that by decreasing the fuel drop size in the air-fuel mixture, fuel consumption of the engine decreased, while heat-release rate and the combustion velocity of the air-fuel mixture increased.

Key words: bioethanol, fuel drop size, spark ignition engine, heat-release rate, combustion pressure.

INTRODUCTION

Since developing the Otto-cycle engine by N.A. Otto, formation of the air-fuel mixture in the spark ignition engines has considerably improved. In the homogeneous mode, used in Otto-cycle engines, the entire combustion chamber is filled with the air-fuel mixture. In the newest technology, direct injection engines, the fuel is injected directly into the engine's cylinder. Thus, not entire combustion chamber is filled with air-fuel mixture. The advantage of forming a stratified air-fuel mixture close to the spark plug electrode is that it can be ignited even at relative air-fuel ratio $\lambda_{afr} > 1$ thus, decreasing the fuel consumption (Bosch, 2006, Ilves & Olt, 2012). Since the quantity of the fuel directed into the cylinder depends above all on the engine load, the decreased fuel consumption using stratified forming of the air-fuel mixture is achieved only in case of the engine's partial load (Bosch, 2006).

Lately, there has been much discussion about using renewable fuels in the transportation sector. One of the most used alternatives to fossil-based fuels is bioethanol. Brazil and USA are among the largest producers of bioethanol in the world. In different standardised bioethanol fuels (e.g. E85) the absolute alcohol is used.

Production of nonstandard bioethanol with high water content is cheaper compared to the standard bioethanol which makes it a feasible alternative to standard bioethanol. Using bioethanol in direct injection spark ignition engines is complicated by the viscosity and lubricating properties of bioethanol (Ma et al., 2004). In particular this concerns nonstandard bioethanol. Thus in case of nonstandard bioethanol fuel, it is more reasonable to use indirect fuel supply systems. In order to decrease the fuel consumption of spark ignition engines with an in-direct fuel supply system, the combustion process should be made more efficient. Efficiency of the combustion process in case of homogeneous air-fuel mixture can be increased by decreasing the fuel drop size. The smaller the size of fuel drops in the air-fuel mixture, the faster the air-fuel mixture evaporates in the cylinder and the higher the combustion velocity of the air-fuel mixture (Farouk & Dryer, 2011). This also gives rise to faster heat release rate per crank angle degree (Williams, 1985). Mathematically, the heat release rate is expressed as follows (Heywood, 1988):

$$\frac{dQ_n}{dt} = \frac{\gamma_{hr}}{\gamma_{hr}-1} \cdot p_c \cdot \frac{dV_c}{dt} + \frac{1}{\gamma_{hr}-1} \cdot V \cdot \frac{dp_c}{dt}, \tag{1}$$

where: Q_n – is the heat amount that is released as the fuel burns in the cylinder; t – time for rotating the crank; γ_{hr} – ratio of specific heats, which in case of ethanol fuel is $\gamma_{hr} = 1.26$ (Kamboj & Kairimi, 2012); p_c – combustion pressure; V_c – cylinder volume.

According to Heywood (1988) the amount of released energy influences the combustion pressure p_c, which can be expressed from the fuel mass combustion rate as follows:

$$p_c = \frac{-\frac{d(m \cdot u)}{dt} + \frac{dQ_{ht}}{dt} + h_{cor} \cdot \frac{dm}{dt}}{\frac{dV_c}{dt}}, \tag{2}$$

where: m – gas mass in cylinder; u – specific internal energy; h_{cor} – heat-transfer coefficient.

From the previous equation (2), we can express the fuel mass combustion rate $\frac{d(m \cdot u)}{dt}$, heat transfer $\frac{dQ_{ht}}{dt}$ and mass flow rate $\frac{dm}{dt}$ as follows:

Heat transfer $\frac{dQ_{ht}}{dt}$ is expressed as:

$$\frac{dQ_{ht}}{dt} = A \cdot h_{cor} \cdot (T_g - T_{wall}), \tag{3}$$

where: A – combustion chamber surface area; T_g – mean combustion gas temperature; T_{wall} – mean cylinder wall temperature,
while heat-transfer coefficient h_{cor} can be expressed with the combustion rate of the heat flux emitted from the cylinder head as follows:

$$\frac{h_{cor} \cdot d_{cb}}{k} = a \cdot \left(\frac{\rho_{afm} \cdot v_p \cdot d_{cb}}{\mu}\right)^b \rightarrow h_{cor} = \frac{a \cdot k \cdot \left(\frac{d_{cb} \cdot v_p \cdot \rho_{afm}}{\mu}\right)^b}{d_{cb}}, \tag{4}$$

where: a – constant of intensity of charge motion $0.35 \leq a \leq 0.8$; b – constant of intensity of charge motion ($b = 0.7$ with normal combustion); k – thermal conductivity;

d_{cb} – cylinder bore; ρ_{afm} – air-fuel mixture density; μ – dynamic viscosity; v_p – piston speed.

The equation (2) is expressed from the first law of thermodynamics in case of an open system

$$\frac{dU}{dt} = \frac{dQ_{ht}}{dt} - p_c \cdot \frac{dV_c}{dt} + \sum_i h_c \cdot m_{fr}, \tag{5}$$

where: $\frac{dU}{dt}$ – the maximum internal energy of system materials, and this relation is valid $\frac{dU}{dt} \approx \frac{d(m \cdot u)}{dt}$; m_{fr} – fuel flow rate and in this case $\frac{dm}{dt} = m_{fr}$, which is expressed as follows:

$$m_{fr} = -\frac{m_c \cdot V_{cp}}{V_c^{\,2}} \cdot \frac{dV_c}{dt} \tag{6}$$

where: V_{cp} – combustion chamber volume; m_c – the mass of the air-fuel mixture that is directed to the cylinder in one work cycle, expressed as follows:

$$m_c = V_c \cdot \rho_{afm}, \tag{7}$$

The combustion rate of one fuel drop $\frac{d(m \cdot u)}{dt}$ is expressed according to F.A. Williams (1985):

$$\frac{d(m \cdot u)}{dt} = -4 \cdot \pi \cdot r_{fd}^2 \cdot \rho_f \cdot \frac{dr_{fd}}{dt}, \tag{8}$$

where: r_{fd} – droplet radius in the air-fuel mixture where $r_{df} = \frac{D_{32}}{2}$; D_{32} – Sauter mean diameter.

To evaluate the mass combustion rate of the entire air-fuel mixture, the equation (8) has to be modified to determine the mass combustion rate of the fuel drops found in the entire air-fuel mixture. For this, one fuel drop mass combustion rate $\frac{d(m \cdot u)}{dt}$ has to be multiplied with the total number of fuel drops, N, in the air-fuel mixture; and to get the heat emitted per unit of time during combustion, multiply it with the fuel calorific value $Q_{f.teor}$.

$$\frac{d(m \cdot u)}{dt} = -4 \cdot \pi \cdot \left(\frac{D_{32}}{2}\right)^2 \cdot \rho_f \cdot \frac{d\left(\frac{D_{32}}{2}\right)}{dt} \cdot Q_{f.teor} \cdot N, \tag{9}$$

where: $Q_{f.teor}$ – fuel calorific value; N – total number of fuel drops in the air-fuel mixture, which is expressed as the ratio of the fuel quantity directed into the cylinder V_f and volume of the fuel drops:

$$N = \frac{V_f}{\frac{4}{3} \cdot \pi \cdot \left(\frac{D_{32}}{2}\right)^3}, \tag{10}$$

where V_f – the fuel quantity directed into the cylinder in one work cycle.

Taking into account equations (3), (4), (6), (7), and (9) and replacing them into equation (2), we get the equation for calculating combustion pressure p_c; with the help of this, the change of combustion pressure p_c can be evaluated from the diameter of the fuel drops in the air-fuel mixture D_{32}. Based on equations (2), (6) and (9), it is a differential equation, which entails two types of derivatives, $\frac{d(\frac{D_{32}}{2})}{dt}$ and $\frac{dV_c}{dt}$. The intensity of fuel drops size change $\frac{d(\frac{D_{32}}{2})}{dt}$ can be deduced from the air-fuel mixture's combustion velocity v_{afm} formula. Therefore, this relation is valid $\frac{d(\frac{D_{32}}{2})}{dt} \approx v_{afm}$, and air-fuel mixture combustion velocity is expressed with the equation (Williams, 1985):

$$v_{afm} = \frac{\lambda}{\rho_{afm} \cdot c_p} \sqrt{4 \cdot \pi \cdot \left(1 + \frac{1}{\lambda_{afr}}\right) \cdot N_k \cdot \frac{D_{32}}{2} \cdot \ln(1 + B)}, \tag{11}$$

where: λ – thermal conductivity; c_p – specific heat at constant pressure; λ_{afr} – stoichiometric fuel-gas ratio; N_k – number of fuel drops per unit volume; B – combustion constant.

The change of cylinder volume at different crankshaft angles of rotation φ can be expressed as a ratio of cylinder volume change and time

$$\frac{dV_c}{dt} = \frac{V_c + \frac{\pi \cdot {d_{cb}}^2}{4} \cdot \left(l + d_{cr} - (d_{cr} \cdot \cos\varphi + \sqrt{l^2 - {d_{cr}}^2 \cdot sin^2\varphi})\right)}{t}, \tag{12}$$

where: d_{cr} – crank radius; l – connecting road length;

following from the above, the combustion pressure p_c calculation model is expressed as follows:

$$p_c = \frac{t}{V_c + \frac{\pi \cdot {d_{cb}}^2}{4} \cdot \left(l + d_{cr} - \left(d_{cr} \cdot \cos\varphi + \sqrt{l^2 - {d_{cr}}^2 \cdot sin^2\varphi}\right)\right)} \cdot \Bigg[4 \cdot \pi \cdot \left(\frac{D_{32}}{2}\right)^2 \cdot \rho_f \cdot \frac{\lambda}{\rho_{afm} \cdot c_p} \cdot$$
$$\sqrt{4 \cdot \pi \cdot \left(1 + \frac{1}{\lambda_{afr}}\right) \cdot N_k \cdot \frac{D_{32}}{2} \cdot \ln(1 + B)} \cdot Q_{f.teor} \cdot N + A \cdot \frac{a \cdot k \cdot \left(\frac{d_{cb} \cdot v_p \cdot \rho_{afm}}{\mu}\right)^b}{d_{cb}} \cdot$$
$$(T_g - T_{wall}) + h_c \cdot -\frac{(V_c \cdot \rho_{afm}) \cdot V_{cp}}{{V_c}^2} \cdot \frac{V_c + \frac{\pi \cdot {d_{cb}}^2}{4} \cdot \left(l + d_{cr} - \left(d_{cr} \cdot \cos\varphi + \sqrt{l^2 - {d_{cr}}^2 \cdot sin^2\varphi}\right)\right)}{t}\Bigg] \tag{13}$$

This formula enables to calculate combustion pressure at the different working modes of the engine, depending on the fuel drop size in the air-fuel mixture. To illustrate Equation 13, a sample graph has been compiled (Fig. 1), which characterises the change of combustion pressure depending on the fuel drop size. Technical data of a spark ignition engine of a regular passenger car were used in the calculations. The calculation results have been transferred to percentages, where $p_{c.max} = 100\%$ and $p_{c.min} = 0$. The range of fuel drop sizes has been chosen $D_{32} = 5\ldots500$ µm.

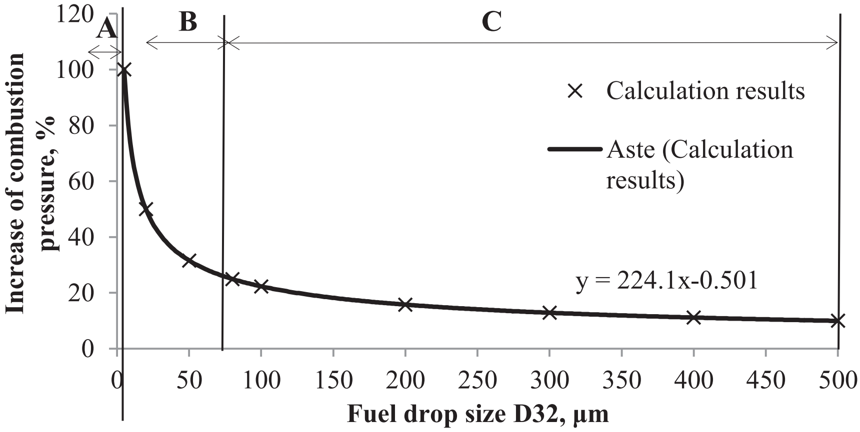

Figure 1. Change of combustion pressure depending on fuel drop size in the air-fuel mixture.

Fig. 1 shows that the combustion pressure increases with the decreasing of the fuel drop size. Furthermore, it can be seen that in the region C ($D_{32} = 80...500$ µm) the change in the increase of combustion pressure is considerably smaller with changing drop size, while in the region B (fuel drop size 80 µm to 20 µm) the combustion pressure increases about twice. When decreasing the fuel drop size below 20 µm (region A), combustion pressure increases drastically, which can cause detonating combustion in the engine's cylinder. Thus, it is important to form the air-fuel mixture with the drop size in the region B in order to enable the controlled combustion in the engine's cylinder.

Using the calculation model (Equation 13), increase of combustion pressure in the fuel drop diameter range of 20…80 µm varied with data from different engines 7…60%. An equation of the curve for the calculated characteristic has been indicated on figure 1 as follows:

$$y = 224.1 \cdot x^{-0.501} \longrightarrow p_c = 224.1 \cdot {D_{32}}^{-0.501}, \tag{14}$$

It enables to evaluate the increase of combustion pressure according to fuel drop size in the air-fuel mixture.

The previous equation (14) characterises combustion pressure p_c change depending on fuel drops' average diameter D_{32}. Decreasing fuel drop size increases the combustion pressure p_c in the cylinder, which is caused by increase of the heat release Q_n in unit of time t.

This article investigates the spark engine's combustion process when using 96.4% bioethanol as a fuel. More precisely, the bioethanol fuel combustion process is observed using a spark ignition engine with a novel fuel supply system, which guarantees the average fuel drops diameter D_{32} of approximately 23 µm in the air-fuel mixture (Olt et al., 2013). It has to be mentioned that in case of a regular spark ignition engine, the average fuel drop size is $D_{32} \approx 80$ µm in E85 bioethanol fuel injection spray (Gandhi & Meinhart, 2008).

MATERIALS AND METHODS

For the formation of the small fuel drop size bioethanol air-fuel mixture, a special fuel supply system has been used. More thorough working description of this fuel supply system has been provided in patent document EE 05665 B1 Olt et al. (2013). At least two pulverisers are used in the fuel supply system. The pulverisers have been placed opposite to one another on the same axis therefore, fuel drops in the sprays collide and fragment even further (Olt et al., 2013).

The fuel supply system that enables the formation of air-fuel mixture with small fuel drop size is referred to as a pulveriser fuel supply system. Fig. 2 illustrates the formation of the air-fuel mixture in the pulveriser fuel supply system.

Formation of the air-fuel mixture with small fuel drop size in the pulveriser fuel supply system is ensured by two-step carburation. The first-step carburation occurs in the pulveriser (Figs 2, 11 and 12) and second-step carburation in the intake manifold, where fuel sprays collide with each other (Figs 2, 14) (Olt et al., 2013). The fuel drop size in the air-fuel mixture of the pulveriser fuel supply system has been measured using Malvern Sprytec STP2911. The fuel supply system of Audi ADR 1.8i test engine was used as a reference. The average fuel drop size D_{32} of the fuel spray formed by the regular fuel supply system was determined on the basis of Gandhi & Meinhart (2008).

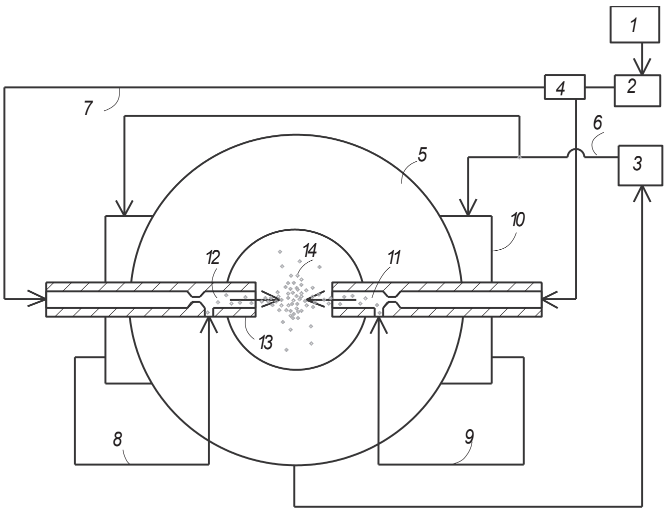

Figure. 2. Schematic of the formation of the air-fuel mixture in a pulveriser fuel supply system (Olt et al., 2013). 1 – compressor; 2 – pressure vessel; 3 – fuel tank; 4 – air-pressure regulator; 5 – system corps; 6 – fuel line to fuel-flow regulator; 7 – air line; 8 and 9 – fuel line to pulveriser; 10 – fuel-flow regulator; 11 and 12 – first-step carburation; 13 – pulveriser; 14 – second-step carburation.

In case of a pulveriser fuel supply system, the engine's intake manifold was modified. With the pulveriser fuel supply system the fuel was injected behind the throttle valve, while with the test engine's original fuel supply system the fuel was injected behind the intake valve. Furthermore, the length of the engine's intake manifold decreased. The general tendency is that in case of a long intake manifold, the cylinder's charging efficiency on the crankshaft's rotational speed n_e = 1,000…5,500 rpm is better or as good as with a short intake manifold (Heisler, 1995). In order to minimize the effect of the length of the intake manifold on engine output parameters, the engine load during the experiments was chosen $T_e = 30$ Nm and crankshaft's rotational speed $n_e = 3{,}000\ldots4{,}500$ rpm.

A modified test bench KI5543 was used during the experiments with the engine load of Te = 30 Nm and crankshaft's rotational speed of ne = 3,950 rpm. As this test bench enables engine break on the bench rotary's rotational speed of $n_d = 1{,}500\ldots3{,}000$ rpm (Hutjuk & Tsehov, 1989), gearbox with the transmission ratio of $\eta_{gb2} = 1.84$ was used during the transmission. The test engine's technical data are indicated in Table 1.

Table 1. Technical data of the Audi 1.8 ADR engine (Olt et al., 2009)

Name	Value
Fuel supply system	MPI-Bosch Motronic M3.2
Cylinder number	4
Cylinder bore, mm	81
Piston stroke, mm	86.4
Volume, cm^3	1781
Cooling system	liquid cooled
Power, kW	92 (5,800 rpm)
Torque, Nm	173 (3,960 rpm)
Compression ratio	10.3
Engine stroke	4
Resisting moment, Nm	26

Combustion pressure in the engine cylinder was measured using AVL 621 and the fuel consumption of the engine using weighing device CAS CI-2001A. The measuring time t of the fuel consumption was 60 s. Based on the combustion pressure, the heat release Q_n and respective heat release rate $\frac{dQ_n}{d\varphi}$ were calculated. Heat release rate was calculated according to Equation 1. Heat release Q_n is expressed as the follows (Heywood, 1988):

$$Q_n = \frac{dQ_n}{d\varphi} + Q_{n.\varphi-1} \tag{15}$$

where: $Q_{n.\phi\text{-}1}$ – the net heat per crank angle degree that was released during the combustion process; φ – crankshaft angle.

Other parameters characteristic to the engine work have been calculated according to the standard GOST 18509-88.

RESULTS AND DISCUSSION

The experimental data shown in Table 2 characterise more precisely the fuel drop size in the air-fuel mixture. D_{10} is the arithmetic mean of the droplet diameter, D_{50} is mass median diameter, where 50% drops have smaller and 50 % bigger diameter, D_{90} is the diameter of drops of which 90% are smaller (Malvren, 2012), D_{32} is Sauter mean diameter, and D_{43} is Herdan mean diameter, which characterises the fuel drop size most frequently found in the injected fuel spray (Sescu, 2011; Malvren, 2012). According to Gandhi et al. (2008) Sauter mean diameter is used to characterise the fuel drop size found in the injection system of a regular spark ignition engine. Therefore, Sauter mean diameter D_{32} was taken as the basis to describe the air-fuel mixture formed in the pulveriser fuel supply system as well. Experiments showed that the average Sauter mean diameter D_{32} in the air-fuel mixture formed by a pulveriser fuel supply system is approximately four times smaller than in the air-fuel mixture formed by the engine's original fuel supply system. The results of engine tests performed with both fuel supply systems are presented in Table 3. The tests were performed at constant engine load and crankshaft's rotational speed. In order determine the impact of the air-fuel mixture on the combustion process, the same ignition angle α_i given by the test engine's original control unit settings was used during testing.

Table 2. The characteristics of air-fuel mixture of 96.4% bioethanol fuel formed by a pulveriser fuel supply system, where D_{10} is the arithmetic mean droplet diameter, D_{50} Mass Median Diameter, D_{90} drop size of which 90% of the fuel drops are smaller (Malvren, 2012), D_{32} Sauter mean diameter, and D_{43} Herdan mean diameter (Sescu, 2011; Malvren, 2012)

Name	Fuel system pressure
D_{10} (μm)	12.22
D_{50} (μm)	57.46
D_{90} (μm)	164.46
D_{32} (μm)	22.53
D_{43} (μm)	75.77

Table 3. Engine testing data using 96.4% bioethanol fuel, where α_i is ignition angle, n_e crankshaft rotational speed, T_e torque, P_e power, B_f fuel consumption, b_e specific fuel consumption, p_e mean effective pressure, p_i indicated pressure, P_i indicated power, b_i indicated specific fuel consumption, η_e engine efficiency and η_i indicator efficiency

Symbol	Unit of measurement	Original fuel supply system	Pulverizer fuel supply system
α_i	deg	33	33
n_e	rpm	3960	3960
T_e	Nm	30.0	30.0
P_e	kW	12.4	12.4
B_f	kg h^{-1}	**14.9**	**14.58**
b_e	g (kWh)$^{-1}$	1200.5	1176.3
p_e	MPa	0.209	0.209
p_i	MPa	0.209	0.209
P_i	kW	23.2	23.2
b_i	g (kWh)$^{-1}$	642.2	629.3
η_e	-	0.112	0.114
η_i	-	0.209	0.214

Table 3 indicates that in the same load regime, when using small fuel drop size air-fuel mixture formed by pulverized fuel supply system, the fuel consumption decreases approximately by 2%. This can be explained by the combustion process analysis. In order to illustrate the fuel consumption decrease, Fig. 3 has been complied based on the experimental data.

Fig. 3 indicates that combustion pressure p_{avg} for the pulverised fuel supply system is higher than for the regular fuel supply system. This results from the faster combustion of the smaller fuel drop size air-fuel mixture in the cylinder. As the maximum combustion pressure p_{max} for the pulverised fuel supply system has been achieved ~5 deg after top dead centre, a situation arises where the combustion pressure starts working against piston rise. From this, it can be deduced that by adjusting the ignition angle it is possible to decrease engine's fuel consumption in the current regime. Comparing the heat release rates of the regular fuel supply system and the pulveriser fuel supply system (*dQ/dϕorig* and *dQ/dϕ pulv*), it can be seen that the maximum heat release rate increases in pulverised fuel supply system approximately 13%, while in regular fuel supply system the heat release lasts longer. Thus, it can be deduced that in case of the air-fuel mixture with smaller fuel drop size, heat is released quicker and therefore, heat release is more intense. In addition, Fig. 3 shows that in case of *dQ/dϕ pulv* heat release begins much earlier than with *dQ/dϕorig,* which also causes a quick rise in combustion pressure and in the combustion velocity of the air fuel mixture in the cylinder. The heat released from the combustion process remains the same in both fuel supply systems, and is defined by the engine load.

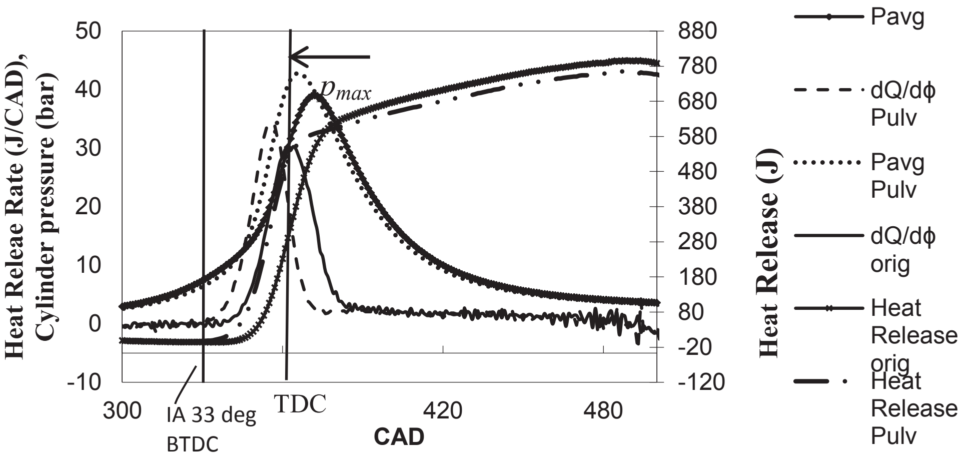

Figure 3. The net-heat rate emitted from the combustion process of Audi 1.8 ADR engine (T_e = 30 Nm, n_e = 3,960 rpm).

Based on the fuel consumption data (Table 3), the heat release rate directed into one cylinder of the engine during one working cycle (pulveriser fuel supply system $\boldsymbol{Q_{n.teor.pulv}}$ = 813 J and original fuel supply system $\boldsymbol{Q_{n.teor.orig}}$= 830 J) can be calculated. By dividing the net heat released during the combustion with theoretical amount of energy in the air-fuel mixture, we get the amount of energy that was absorbed by cylinder walls. In case of the pulveriser fuel supply system, approximately ~3% more energy was absorbed than in regular fuel supply system. As more energy is absorbed by the cylinder walls, more energy will be available for the fuel drops to evaporate. Therefore, the air-fuel mixture with smaller fuel drop size evaporates faster thus causing quicker and more complete combustion of the air-fuel mixture in the cylinder.

CONCLUSIONS

Results indicate that use of the air-fuel mixture with small fuel drop size causes an increase in combustion pressure p_c and heat release Q_n, and therefore a decrease in engine's fuel consumption. In the current case, bioethanol consumption decreased approximately by 2%. The fuel consumption could be further decreased by optimising the ignition angle. Moreover, the air-fuel mixture with small fuel drop size causes faster evaporation, which also facilitates faster heat release and ~3% more energy absorbed by the cylinder walls.

As an extension study, it is recommended to conduct experiments with a previously adjusted engine, where the ignition angle is optimal with both air-fuel mixtures, and study the combustion of the air-fuel mixture on the engine's full load regime.

REFERENCES

Bosch, R. 2006. GmbH. Gasoline-engine management. Chichester, John Wiley & Sohn Ltd, Germany.

Farouk, T. & Dryer, F.L. 2011. Studies of the combustion of drops in a fuel spray the burning of single drops of fuel. *Combustion Theory and Modelling* **15**(4), 487–515.

Gandhi, A.H. & Meinhart, M.A. 2008. Comparison of Measured PFI Spray Characterizations of E85 and N-heptane *Fuels for a Flex-Fuel Vehicle. ILASS Americas, 21st Annual Conference on Liquid Atomization and Spray Systems*, Orlando, Florida.

Heisler, H. 1995. Advanced engine technology. London, UK, Planta Tree.

Heywood, J.B. 1988. Internal Combustion Engine Fundamentals. McGraw-Hill. 930 pp.

Hutjuk, V.A. & Tsehov E.S. 1989. Practical work on auto-tractor engines. Russian. Minsk, Uradzhai, 143 pp.

Ilves, R. & Olt, J. 2012. Study of prior art of spark ignition engine fuel supply system. *Agronomy Research* **10**(1), 55–74.

Kamboj, K.S. & Kairimi M.N. 2012 Effects of Compression Ratios, Fuels And Specific Heats On The Energy Distribution in Spark-Ignition Engine. International Journal of Emerging Technology and Advanced Engineering. ISSN 2250-2459, Volume **2**, Issue **8**, 482–491.

Ma, X.Q., DeCarmine, T. & Xiao, T.D. 2004. Plasma Spray High Lubricity Nanocomposite Coatings. Thermal Spray 2004, Advances in Tehnology and Application.

Malvren. 2012. A Basic Guide to Particle Characterization. Available: http://golik.co.il/Data/ABasicGuidtoParticleCharacterization%282%29_1962085150.pdf pdf (19.11.2013).

Olt, J., Küüt, A. & Ilves, R. 2013. Patent No: EE05665A2. Formation method of fule-air mixture of reciprocating engine and flexible-fuel system. Ht.ee. F02B 47/04, F02D 19/08, F02M 43/04, F23K 5/12.

Olt, J., Mikita, V., Sõõro, T., Küüt, A., Tamm, E., Raidla, E. & Ritslaid, K. 2009. Mixture of bioethanol and gasoline as Otto motor fuel. Energy efficiency and agricultural engineering. ISSN 1311–9974, 591–600.

Sescu, C. 2011. Experimental and Computational Study on Liquid Atomization by Slinger Injector. Submitted to the Graduate Faculty as partial fulfillment of the requirements for the Doctor of Philosophy Degree in Engineering. The University of Toledo, Spain.

Williams, F.A. 1988. Combustion Theory. The Fundamental Theory of Chemically Reacting Flow System. Second Edition. The Benjamin/Cummings Publishing Company, Inc. USA.